

Bond deterioration effects on corroded RC bridge pier in seismic zone

*Original*

Bond deterioration effects on corroded RC bridge pier in seismic zone / Bartolozzi, M.; Casas, J. R.; Domaneschi, M.. - In: STRUCTURAL CONCRETE. - ISSN 1464-4177. - STAMPA. - (2021), pp. 1-16. [10.1002/suco.202000681]

*Availability:*

This version is available at: 11583/2940532 since: 2021-11-26T12:02:14Z

*Publisher:*

John Wiley and Sons Inc

*Published*

DOI:10.1002/suco.202000681

*Terms of use:*

openAccess

This article is made available under terms and conditions as specified in the corresponding bibliographic description in the repository

*Publisher copyright*

(Article begins on next page)

## ARTICLE

# Bond deterioration effects on corroded RC bridge pier in seismic zone

Mara Bartolozzi<sup>1</sup> | Joan R. Casas<sup>2</sup>  | Marco Domaneschi<sup>1</sup> 

<sup>1</sup>Department of Structural, Geotechnical and Building Engineering, Politecnico di Torino, Turin, Italy

<sup>2</sup>Department of Civil and Environmental Engineering, Universitat Politècnica de Catalunya, Barcelona, Spain

## Correspondence

Marco Domaneschi, Department of Structural, Geotechnical and Building Engineering, Politecnico di Torino, Corso Duca degli Abruzzi, 24, 10129 Turin (TO), Italy.  
Email: marco.domaneschi@polito.it

## Abstract

The effects of corrosion focusing on the consequences of bond strength deterioration for a reinforced concrete bridge pier in a seismic affected area are examined in this research. A bond degradation model based on the local bond stress-slip model presented in FIB Model Code 2010 is chosen. A motorway overpass object of a previous study, which considered the rebars cross-section reduction effect only, has been selected to assess the seismic capacity of the corroded pier in the time domain when bond degradation due to corrosion is also taken into account. The modification of strength capacity and ductility of the structural element is analyzed and the effect of corrosion during the whole service life of the structure is obtained. It is concluded that the effect of bond degradation is more critical for the safety of the pier than the effect of rebars cross-section loss.

## KEYWORDS

bond strength, bridges, corrosion, reinforce concrete

## 1 | INTRODUCTION

Despite structures inevitably undergo to deterioration, which intensity depends on environmental conditions and the quality of the materials, an effective design, monitoring, and continuous targeted maintenance interventions can ensure the functionality and the safety of the structure for a long time.

Focusing on reinforced concrete (RC) structures, corrosion of steel reinforcements reasonably represents the main reason for the shortening of their service life.

The three main effects of steel rebars corrosion are the reduction of the rebar cross-section, the cracking of the concrete cover, and the decrease of the bond strength.<sup>1</sup> The use of a truthful bond strength degradation model represents the way to predict the evolution of the structure's strength and ductility over time and to be able to intervene before having a high level of damage or even the collapse of the structure. Therefore, it can be a critical tool for planning intervention and repair operations in efficient maintenance strategies.

Corrosion is an electrochemical process, which consists of the transformation of iron into iron oxides, characterized by increasing volume and low mechanical properties that accumulate in the interface between steel and concrete. In this way, the bond strength is threatened both for the presence of an additional weak

Discussion on this paper must be submitted within two months of the print publication. The discussion will then be published in print, along with the authors' closure, if any, approximately nine months after the print publication.

This is an open access article under the terms of the Creative Commons Attribution-NonCommercial-NoDerivs License, which permits use and distribution in any medium, provided the original work is properly cited, the use is non-commercial and no modifications or adaptations are made.

© 2021 The Authors. *Structural Concrete* published by John Wiley & Sons Ltd on behalf of International Federation for Structural Concrete.

layer between the two materials, the reduction of the mechanical bond interlocking because of the decrease of the rib height, and for the formation of cracks due to the radial pressure created by the high volume oxides. The mechanisms that contribute to bonding are chemical adhesion (at low stress level), friction, and mechanical interaction (high stress level) between the steel and the concrete.<sup>2</sup> Bond strength is influenced by the concrete cover/bar diameter ratio, the type of concrete, and the steel confinement. These factors influence the bond failure type too, which can occur for splitting or pull-out. The first one leads to the formation of cracks in concrete and to the slipping of the rebar. Differently, the pull-out failure is characterized by the crushing of the concrete around the bar without cracks formation, and it usually occurs in case of good confinement.<sup>3</sup>

One of the first studies regarding the corrosion effect on the steel-concrete bond strength was carried out by Al-sulaimani et al.,<sup>4</sup> which demonstrates that in correspondence to low level of corrosion there is an initial increase of the bond strength due to the pressure created by the expansive iron oxides before the cracking of the concrete cover. Such a result was confirmed by many authors, for example, References 5 and 6. Moreover, researches proved that confined concrete exhibits less reduction in the bond strength respect to the unconfined case.<sup>5</sup> Chung et al.<sup>7</sup> performed tests on flexural slabs with corroded reinforcement and the results showed that the decrease of moment capacity is mainly due to the deterioration of the bond between concrete and steel bars and secondarily to the loss of their cross-sectional area. Several of the early models that have been developed to represent the bond strength reduction in corroded structures do not consider the initial increase in bond strength, the stirrups and concrete cover confinement and the influence of the position of longitudinal reinforcement.<sup>5,8</sup> Recent models are characterized by higher accuracy and the capability to take into account several influencing factors.<sup>9,10</sup> Moreover, many models<sup>5,11–13</sup> are based on the relationship between bond strength and surface cracks width that was proved to be a valid indicator of the corrosion bond degradation.

This research focuses on the determination of the bond strength deterioration effect on the seismic capacity of an RC bridge pier. The results are compared with those from a previous research<sup>14,15</sup> that designed the structure and developed a similar study based on the reinforcement area reduction effect only. The bond strength model chosen for the present research development is ARC2010,<sup>16</sup> as considered the most complete among the several analyzed for anchorage assessment in concrete structures with corroded reinforcements. Through interaction and Bresler's domains the effects of bond

deterioration on the strength capacity of the pier have been evaluated, and a comparison with the results of the previous research (i.e.,<sup>14,15</sup>) is carried out. Moreover, the ductility of the element is checked plotting moment-curvature diagrams, considering and neglecting the bond strength reduction effect, in addition to the corrosion induced steel area loss.

## 2 | BRIDGE CASE STUDY

The bridge considered for the study is a motorway overpass located in Sicily, close to the strait of Messina, zone of high seismic hazard. A complete description of the geometry, structural conditions, and the seismic loading characterization can be found in References 14 and 15. However, in order to make the manuscript self-contained, some key general aspects are summarized below.

### 2.1 | The bridge structure and the adopted finite element model

The structure is 55.5 m in length and consists of two spans, each one of 27.75 m. The deck is a solid slab in prestressed concrete with lightnings and variable depth (Figure 1, left). The bridge pier with “Y” shape is 6.70 m high and is the object of the present study. At the pier and the bents, support devices (elastomeric bearings) have been adopted. The foundation consists in a  $5 \times 5 \times 2.5$  rigid footing. The selected construction materials are Steel B450C and Concrete C40/50.<sup>15</sup>

The two-span bridge has been implemented in SAP2000 as continuous beam, and a suitable finite element (FE) model has been created to perform the seismic analysis (Figure 1, right). The adopted discretization of each span considers six different sections. The Y-shaped pier has been modeled by frame elements: the two arms and the vertical shaft have been discretized in four different sections. The deck and the pier have been connected by the neoprene pads using rigid body constraints.<sup>15</sup>

### 2.2 | Seismic analysis

The bridge construction site belongs to the high seismic hazard area close to the Strait of Messina in Sicily (Italy). Indeed, it is classified as the first seismic category, associated by the highest seismic intensity, among four, by the current Italian standard for constructions NTC2018.<sup>17</sup> The seismic analysis has been performed as static linear analysis to verify the strength capacity of the individual structural elements and the whole structure, according to

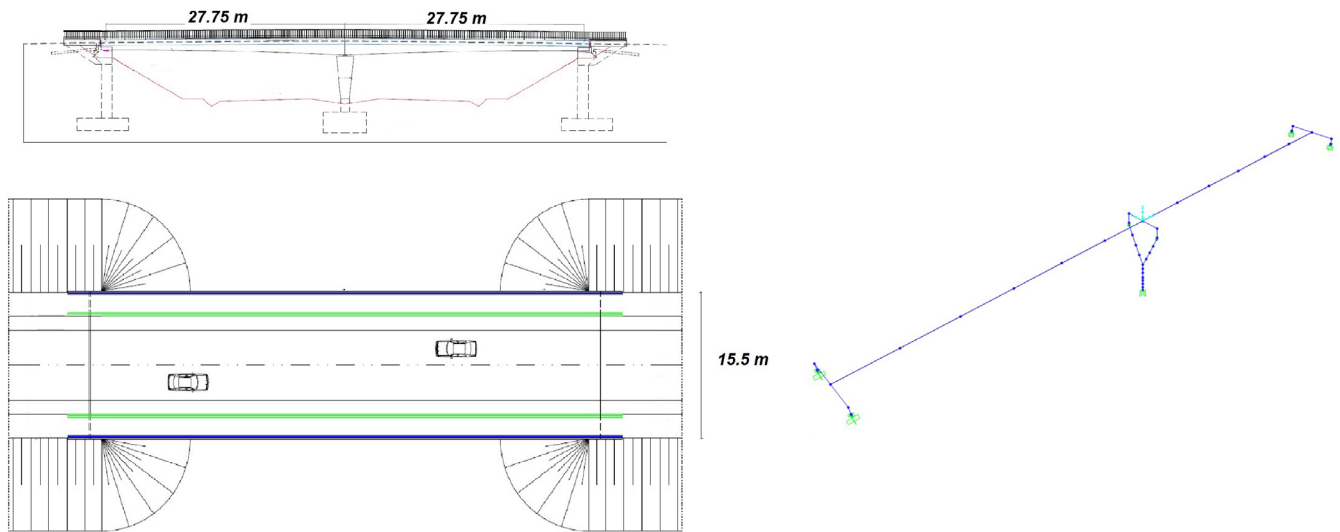


FIGURE 1 Bridge structure (left) and the FE model (right)

the demand actions associated to the SLV (life-saving limit state), the ultimate limit state for NTC2018.<sup>17</sup> The ductile behavior for the cross sections of the structural elements is prescribed and the “capacity design” criterion has been used. The design response spectra have been defined adopting the adequate behavior factor  $q$ . With this respect, the resulting peak ground accelerations in the horizontal and vertical directions result 0.332 g and 0.258 g, respectively.<sup>14,15,17</sup> The earthquake parameters have been the used in SAP2000 as “response spectrum” load.

The seismic loads combination has been finally applied to the bridge computing the values of internal forces, that is, the axial forces, the bending moments and shears, at the two most critical sections of the “Y” shape pier, section A (base of the pier) and section B (base of the bifurcation) (Figure 2). Subsequently, the dimensioning of the longitudinal and transversal steel reinforcements have been performed following the Italian regulation<sup>17</sup> and the capacity design criteria.<sup>14,15</sup>

### 3 | CORROSION MODEL

The implemented corrosion models refer to those ones adopted in a previous paper<sup>15</sup> of this research group, on the same case study, which considered the rebars cross-section reduction effect only. Some key aspects are summarized below to explain the modeling of metal bars cross-section losses. More details can be found referring to.<sup>15</sup>

Corrosion of embedded steel bars affects RC structures and can be distinguished into two types: *general* and *pitting*. The first one is characterized by a roughly uniform and extensive metal loss over the reinforcing bar, while the second one is concentrated in small areas with higher steel area losses. Pitting corrosion mainly occurs in chloride environments, therefore if the structure is located in a marine environment, both corrosion types may occur in association.<sup>18</sup>

The effect of the corrosion process on the steel bar is quantified with reference to the method presented in

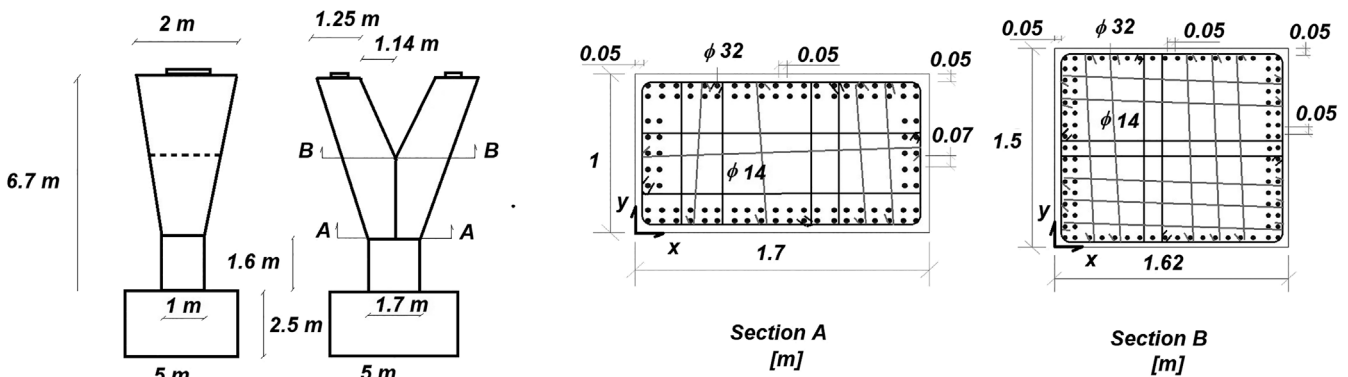


FIGURE 2 Bridge pier geometry with steel reinforcements details for sections A and B

	Pull out	Splitting – Unconfined	Splitting – Stirrups
$\tau_{b,max}$ (MPa)	$2.5 \sqrt{f_{cm}}$	$2.5 \sqrt{f_{cm}}$	$2.5 \sqrt{f_{cm}}$
$\tau_{bu,split}$ (MPa)	/	Equation (8)	Equation (8)
$s_1$ (mm)	1	$s_{\tau_{bu,split}}$	$s_{\tau_{bu,split}}$
$s_2$ (mm)	2	$s_1$	$s_1$
$s_3$ (mm)	$c_{clear}$	$1.2 s_1$	$0.5 c_{clear}$
$\alpha$	0.4	0.4	0.4
$\tau_{res}$ (MPa)	$0.4 \tau_{b,max}$	0	$0.4 \tau_{bu,split}$

TABLE 1 Parameters for local bond stress-slip curve for MC 2010 “good bond conditions”

Reference 19, where the residual reinforcement diameter  $d(t)$  is computed by Equation (1), the residual pitting depth  $p(t)$  at time  $t$  (assumed to take a hemispherical form) by Equation (2), and the residual cross-sectional area of steel bar  $A(t)$  due to general corrosion by Equation (3).<sup>15</sup>

$$d(t) = d_0 - 2 \int_{t_{corr}}^t \lambda(t) dt, \quad (1)$$

$$p(t) = R \int_{t_{corr}}^t \lambda(t) dt, \quad (2)$$

$$A(t) = \frac{\pi}{4} [d(t)]^2. \quad (3)$$

In Equations (1)–(3), the parameter  $d_0$  is the diameter of the intact reinforcement bar,  $R$  the amplification factor representing the ratio between maximum and uniform corrosion penetration,  $\lambda(t)$  the corrosion rate function.<sup>15</sup>

## 4 | BOND DETERIORATION MODEL

ARC2010 bond degradation model is based on the local bond stress-slip model presented in Model Code 2010.<sup>20</sup> The local bond stresses are computed as a function of the relative displacement (slip) parallel to the bar axis and presented in the following Equations (4)–(7), while related parameters for different failure modes are reported in Table 1, where  $\tau_b$  is the tangential bond strength (MPa),  $\tau_{b,max}$  the maximum value of the tangential bond strength (MPa),  $\tau_{res}$  the residual tangential bond strength (MPa) (after splitting or pull-out and with stirrups confinement; without stirrups  $\tau_{res} = 0$ ),  $s$  (1,2,3) the slip values with respect to local bond strength,  $\tau_{bu,split}$  the tangential bond splitting strength (MPa),  $f_{cm}$  the mean cylinder compressive strength (MPa),  $c_{clear}$  the clear distance between ribs (mm) (ARC2010<sup>16</sup>).

$$\tau_b = \tau_{b,max} \left( \frac{s}{s_1} \right)^\alpha \text{ for } 0 \leq s \leq s_1, \quad (4)$$

$$\tau_b = \tau_{b,max} \text{ for } s_1 \leq s \leq s_2, \quad (5)$$

$$\tau_b = \tau_{b,max} - (\tau_{b,max} - \tau_{res}) (s - s_2) / (s_3 - s_2) \text{ for } s_2 \leq s \leq s_3, \quad (6)$$

$$\tau_b = \tau_{res} \text{ for } s_3 \leq s. \quad (7)$$

ARC2010 bond degradation model allows for a complete representation of several scenarios. Indeed, different analytical expressions are provided for the computation of the bond strength, differentiating between cracked and un-cracked concrete cover. Both, pull-out and splitting failure can be represented and, in addition, the absence / presence of stirrups and their degree of corrosion can be considered. Several configurations can be truthfully represented thanks to the possibility to take into account the position of the longitudinal steel bar with respect to the RC element cross-section. In ARC2010 the expression used to compute the splitting strength for corrosion level below the cracking limit comes from Model Code 2010 (Equation (8)), while in the case of corrosion-induced cracking of the concrete cover a reduced bond splitting strength is considered (Equation (9)). Moreover, the residual bond stress has been modified for the case of low stirrup content (Equation (10)) and an equivalent slip is considered to take into account corrosion.<sup>16</sup>

$$\tau_{bu,split} = \eta_2 * 6.5 * \left( \frac{f_{cm}}{25} \right)^{0.25} * \left( \frac{25}{\phi_m} \right)^{0.2} \left[ \left( \frac{c_{min}}{\phi_m} \right)^{0.25} \left( \frac{c_{max}}{c_{min}} \right)^{0.1} + k_m * K_{tr} \right], \quad (8)$$

$$\tau_{bu,split,red} = \eta_2 * 6.5 * \left( \frac{f_{cm}}{25} \right)^{0.25} * \left( \frac{25}{\phi_m} \right)^{0.2} (1 + k_m * K_{tr}), \quad (9)$$

$$\tau_{\text{res,mod}}(K_{tr}) = \begin{cases} (0.16 + 12K_{tr}) * \tau_{\text{bu,split,red}} & \text{for } 0 \leq K_{tr} \leq 0.02 \\ 0.4 * \tau_{\text{bu,split,red}} & \text{for } 0.02 < K_{tr} \end{cases} \quad (10)$$

Adopted variables in Equations (8)–(10) are explained in the following:

- $\eta_2$  is 1 for “good bond conditions” (bars with inclination of  $45^\circ$ – $90^\circ$  respect to the horizontal ones during concreting and to those ones with inclination lower than  $45^\circ$  but at a distance up to 250 mm from the bottom and at least 300 mm from the top of the concrete layer) and 0.7 for “all other bond conditions”;
- $\phi_m$  diameter of the anchored bar (mm);
- $k_m$  confinement coefficient (12 for bars within  $5\phi_m \leq 125$  mm from a stirrup corner, 6 if  $c_s > 8c_y$ , and 0 if  $c_s < 8c_y$  or if a crack can propagate to the concrete surface without crossing transverse links;

$$c_{\text{min}} = \min(c_s/2, c_x, c_y);$$

$$c_{\text{max}} = \max\left(\frac{c_s}{2}, c_x\right);$$

- $c_s$  clear spacing between main bars (mm);
- $c_x, c_y$  cover in x and y directions (mm);

**TABLE 2** Cross-section properties and ARC2010 model parameter for sections A and B

$f_{\text{cm}}$ (MPa)	48
$c_s$ (mm)	50
$c_x$ (mm)	50
$c_y$ (section B) (mm)	50
$n_t$ (section A, x)	6
$n_t$ (section A, y)	4
$n_t$ (section B)	4
$n_b$ (section A, x)	20
$n_b$ (section A, y)	9
$n_b$ (section B, x)	18
$n_b$ (section B, y)	17
$c_{\text{clear}}$ (mm)	5.8
$s_t$ (mm)	60
$c_{\text{min}}$ (section A) (mm)	25
$c_{\text{min}}$ (section B) (mm)	25
$c_{\text{max}}$ (mm)	50
$k_m$	12

- $K_{tr}$  amount of transverse reinforcement =  $n_t A_{st} / (n_b \phi_m s_t) \leq 0.05$ ;
- $n_t$  number of legs of confining reinforcement crossing a potential splitting-failure surface at a section;
- $A_{st}$  cross - sectional area of one leg of a transverse bar ( $\text{mm}^2$ );
- $s_t$  longitudinal spacing of confining reinforcement (mm);
- $n_b$  number of anchored bars or pairs of lapped bars in the potential splitting surface.

## 5 | CORROSION, BOND DETERIORATION, AND THE BRIDGE CASE STUDY

### 5.1 | Slip-bond strength relationship

The slip - bond strength relationship has been obtained for section A and B in the direction x and y considering three different cases: (i) pull-out failure, (ii) splitting failure in absence of stirrups, and (iii) splitting failure in presence of stirrups. Table 2 reports ARC2010 model parameters for sections A and B.

As an example, Figure 3 shows the bond-slip curve of section A in x direction (Ax). All the values refer to the instant  $t = 0$  (uncracked concrete) when the corrosion attack did not start yet. The amount of transversal reinforcement is an input parameter of the model, assuming that is subjected to the same corrosion deterioration rate as the longitudinal steel reinforcement. Therefore, different bond-slip curves per each corrosion level are verified. The reduction of the cross - sectional area of the

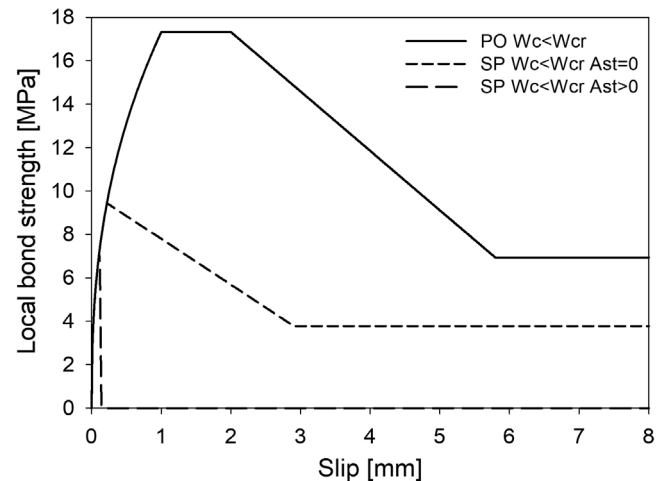


**FIGURE 3** Bond strength – Slip relationship ARC2010 model for section A, x direction ( $t = 0$ ) (continuous line = pull-out failure, long-dashed line = splitting failure in absence of stirrups, short-dashed line = splitting failure in presence of stirrups)

**TABLE 3** Variation of the bond strength for different degree of corrosion of the stirrups in section Ax

$t$ (years)	$A_s(t)$ (General) (mm <sup>2</sup> )		$\tau_{bu,split}$ (General) (MPa)		$A_s(t)$ (Pitting) (mm <sup>2</sup> )		$\tau_{bu,split}$ (Pitting) (MPa)		$A_s(t)$ (G + P) (mm <sup>2</sup> )		$\tau_{bu,split}$ (G + P) (MPa)	
	$K_{tr}$		$K_{tr}$		$K_{tr}$		$K_{tr}$		$K_{tr}$		$K_{tr}$	
0	154.00	0.0241	9.4412		154.00	0.0241	9.4412		154.00	0.0241	9.4412	
10	153.04	0.0239	9.4282		154.00	0.0241	9.4412		153.04	0.0239	9.4282	
20	148.06	0.0231	9.3046		152.66	0.0239	9.4229		146.72	0.0229	9.3418	
30	142.12	0.0222	9.2235		148.45	0.0232	9.3098		136.57	0.0213	9.1477	
40	136.95	0.0214	9.1529		142.51	0.0223	9.2287		125.46	0.0196	8.9960	
50	132.16	0.0207	9.0875		135.42	0.0212	9.1320		113.58	0.0177	8.8338	
60	127.95	0.0200	9.0300		127.38	0.0199	9.0221		101.33	0.0158	8.6664	
70	123.93	0.0194	8.9750		119.33	0.0186	8.9123		89.26	0.0139	8.5016	
80	120.10	0.0188	8.9227		110.52	0.0173	8.7919		76.62	0.0120	8.3290	
90	116.46	0.0182	8.8730		101.33	0.0158	8.6664		63.78	0.0100	8.1537	
100	113.20	0.0177	8.8286		92.13	0.0144	8.5408		51.33	0.0080	7.9837	

longitudinal reinforcement is considered as in Reference 14 and it is assumed equal for the stirrups. Once the variation of the stirrups area in time is known, the bond splitting strength has been computed for different value of  $K_{tr}$ , the parameter that takes into account the amount of transversal reinforcement. The computation has been performed for the two cross sections in both  $x$  and  $y$  directions and for both *general* and *pitting* corrosion. They are characterized by different area reduction in time domain. Moreover, the coupled condition of general and pitting corrosion acting at the same time has been considered. Table 3 reports as an example the variation of the bond strength for different degree of corrosion of the stirrups for section Ax.

## 5.2 | Deteriorated bond strength

The local bond stress-slip curve of corroded reinforcement is approximated shifting the uncorroded curve in the slip direction and considering the minimum value of both, the original and the shifted curve. The additional slip used to shift the curve is the equivalent slip that can be correlated with the corrosion level (in RC elements with stirrups) according to the following equation for the equivalent slip  $S_{eq, stir}$  (mm) as function of the corrosion level (steel weight loss)  $W_c$ :

$$S_{eq, stir} = 13.6 W_c. \quad (11)$$

Once the equivalent slip is computed, the bond strength-slip curves have been translated in order to find the intersection point between the original curve and the new one, representing the deteriorated bond strength at a

specific corrosion level. According to experimental results, it is assumed that the cracking of the concrete cover occurs at a corrosion level of 2%. Then the reduction of bond strength in time domain has been computed for section A and B in both  $x$  and  $y$  directions and has been compared with the steel area reduction in time. The resulting decrease is emphasized during the whole service life of the structure for both the considered corrosion attacks (general and pitting). Reductions occur during the corrosion propagation phase, after the steel depassivation, so during the first years no area and bond strength loss are verified. The comparison plots for section Ax in the cases of general, pitting, and general + pitting corrosion are reported in Figures 4–6. They emphasize how bond degradation is the most demanding effect of corrosion in the RC bridge pier.

## 5.3 | Cross-sectional losses due to general and pitting corrosion

The effect of corrosion of the cross-sectional area losses have been investigated in detail in Reference 15 for longitudinal rebars. The general outcomes have been summarized by Table 4 with deteriorated bond strength for section Ax. When general and pitting corrosion are considered separately, their effects in terms of area losses are roughly comparable, even if pitting is more demanding. However, the worst case is represented by their associated effect. Similar outcomes can be highlighted also by considering the resulting deteriorated bond strength: with the association of both general and pitting corrosion determine the most dangerous condition, with respect to their separate effects. Results for sections Ay, Bx, By are

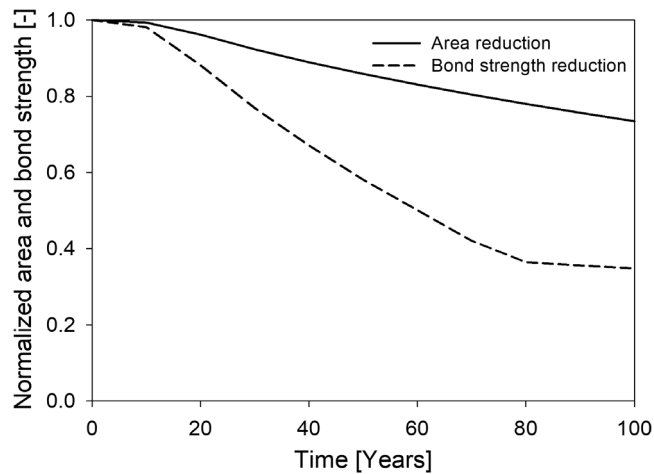


FIGURE 4 Comparison between area and bond strength reduction (general corrosion - section Ax)

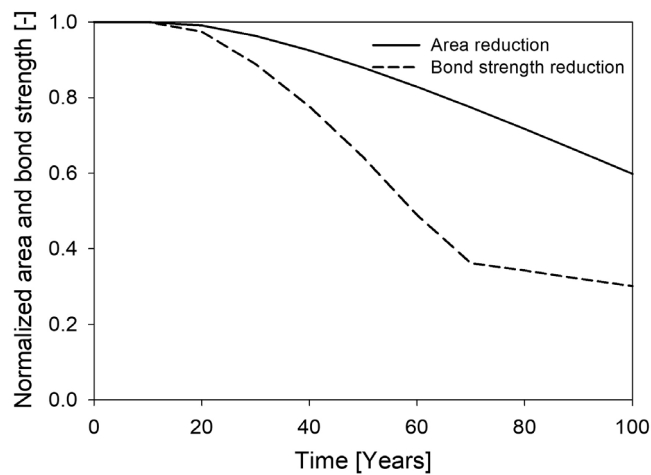


FIGURE 5 Comparison between area and bond strength reduction (pitting corrosion - section Ax)

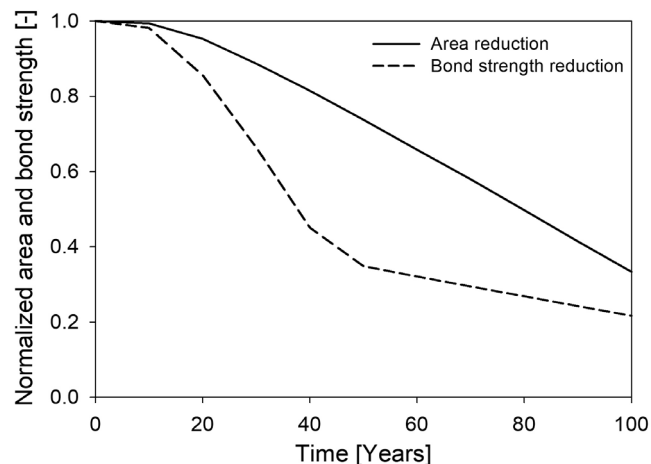


FIGURE 6 Comparison between area and bond strength reduction (general + pitting corrosion - section Ax)

not shown for the sake of brevity since the values are slightly different due to the different reinforcement and geometry but the reduction in adhesion does not change significantly.

## 6 | STRUCTURAL CAPACITY AND DUCTILITY

### 6.1 | Interaction domains

Interaction domains are used to assess the seismic performance of the bridge pier that results simultaneously subjected to axial and bending stresses. The input parameters for the construction of the interaction domains that have been modified to consider the effects of corrosion are steel rebar cross-section, steel yield strength, and steel ultimate strain.<sup>14,15</sup> Therefore, the reductions along time of the three input parameters have been computed for the cases of general corrosion, pitting corrosion, and their coupled effect.

In order to take into account in the present study the effect of bond strength degradation in the cross-sectional capacity, the following hypothesis has been made. It is assumed that, according to an optimal design, the initial bond strength in the undamaged state, taking into account the anchorage length or the lap splice of the rebars, is that one able to bond the rebar working at the yield strength. Due to the degradation of the bond strength with increasing corrosion, the yield strength in the rebar cannot be anymore accommodated by the rebar. Consequently, it has been assumed that the percentage reduction in the bond strength is the same in the maximum tensile strength that the reinforcing steel can develop. So, the degradation of the bond strength, that prevents the material to reach the yielding point and to exhibit a plastic behavior, is modeled by decreasing proportionally the maximum steel strength and the corresponding strain in the linear-elastic part of the stress-strain relationship. In other words, the same decrement that undergoes the bond strength has been considered for the steel yield strength, assuming null post-yielding stiffness, and the maximum strain has been fixed accordingly. This assumption has been experimentally validated as shown at Section 7.

Figures 7–12 show the interaction domains comparing the outputs of the previous study<sup>15</sup> and the present one, for cross sections Ax and By at 0, 20, 40, 60, 80, and 100 years, in the cases of general, pitting, and general + pitting corrosion. The new domains, show that the decrease in adherence strongly affects the structural capacity of the pier. Comparing the resistant domains, a substantial reduction can be observed when the bond



**TABLE 4** Cross-section losses and deteriorated bond strength due to general and pitting corrosion for section Ax

$t$ (years)	General corrosion		Pitting corrosion		G + P corrosion	
	$A(t)$ (mm <sup>2</sup> )	Deteriorated bond strength (MPa)	$A(t)$ (mm <sup>2</sup> )	Deteriorated bond strength (MPa)	$A(t)$ (mm <sup>2</sup> )	Deteriorated bond strength (MPa)
0	804	9.44	804	9.44	804	9.44
20	773	8.32	797	9.2	766	8.08
40	715	6.34	744	7.33	655	4.26
60	668	4.74	665	4.63	529	3.03
80	627	3.44	577	3.23	400	2.53
100	591	3.29	481	2.84	268	2.04

strength deterioration is considered. Section Ax and By are those undergoing an early failure.

## 6.2 | Bresler's domains

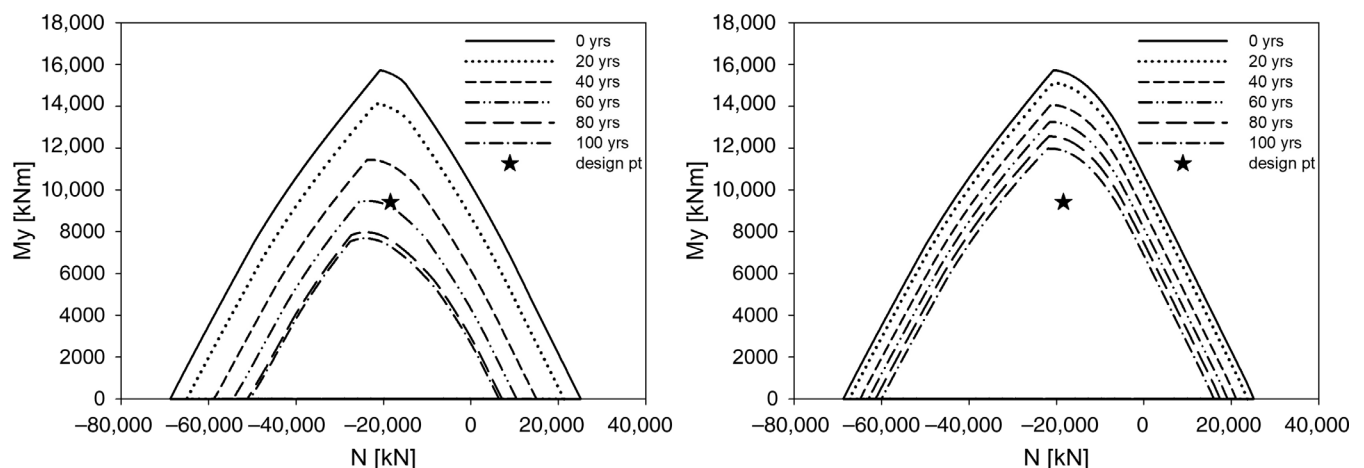
Bresler's domains allow to evaluate the capacity of the structural elements subjected to biaxial bending and axial load. The 2D plots have been obtained for a fixed value of axial load (maximum load acting on the considered section) and present the resistant moments in y and x directions. The resulting domains are strongly reduced if the effect of bond deterioration is considered. The Bresler's domains obtained from the previous study<sup>15</sup> (100 years NB = no bonding effect) and those ones computed in the present study have been compared for the three corrosion cases and both sections A and B (Figures 13–15). The largest continuous line represents the domain of the no corroded section. The medium and the smallest dashed ones represent the

resistant domains after 100 years, considering the steel bars area loss effects and the area loss with bond strength reduction effects, respectively.

Early failure of section A is expected when subjected to all different types of corrosion conditions if the degradation of bond strength is considered, while it occurs only in the case of pitting and general corrosion acting simultaneously if steel area loss effect only is taken into account. Differently, the results highlight an early failure of section B for any corrosion attack typology with and without considering bond degradation effects.

## 6.3 | Moment-curvature diagrams

Apart from strength, also ductility of the cross-sections is also a fundamental property for concrete structures located in seismic zones. In seismic design, ductility is an indicator of the capability to reach high level of


**FIGURE 7** Interaction domain my-N of section A due to general corrosion considering (left) and neglecting (right) bond reduction effect

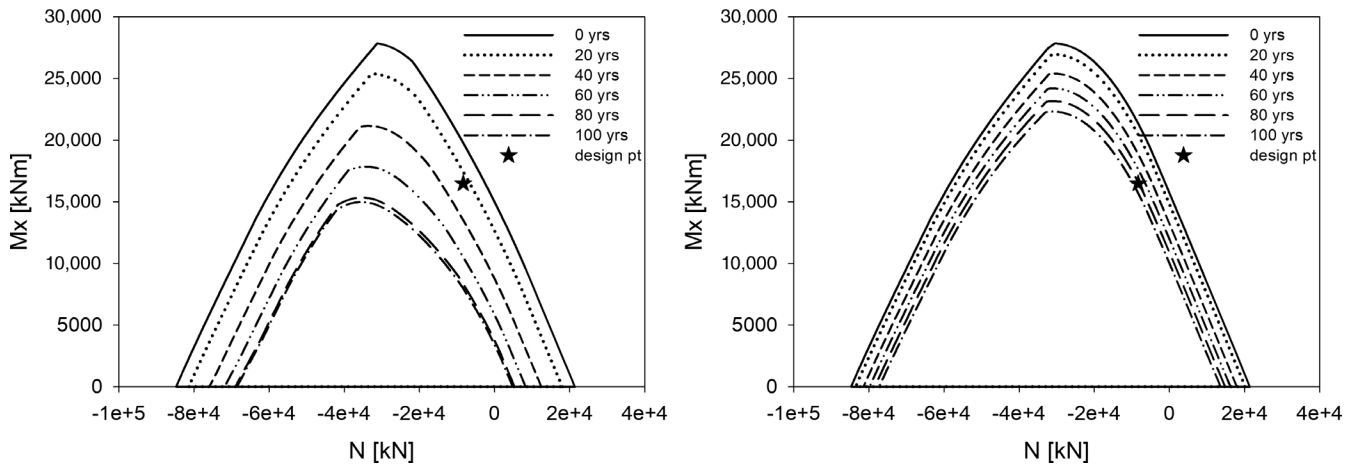


FIGURE 8 Interaction domain  $m_x$ - $N$  of section B due to general corrosion considering (left) and neglecting (right) bond reduction effect

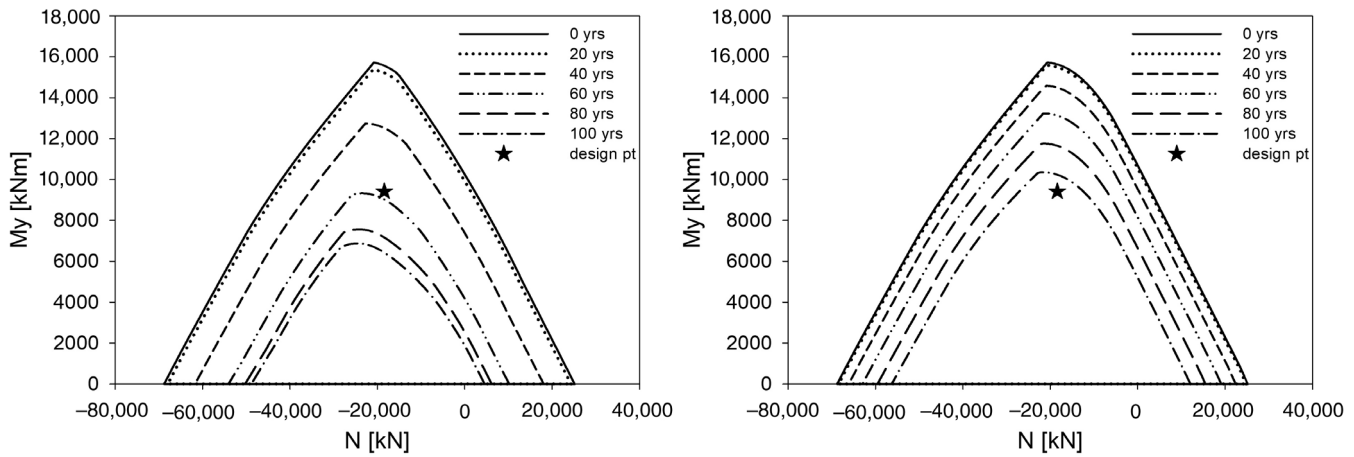


FIGURE 9 Interaction domain  $m_y$ - $N$  of section A due to pitting corrosion considering (left) and neglecting (right) bond reduction effect

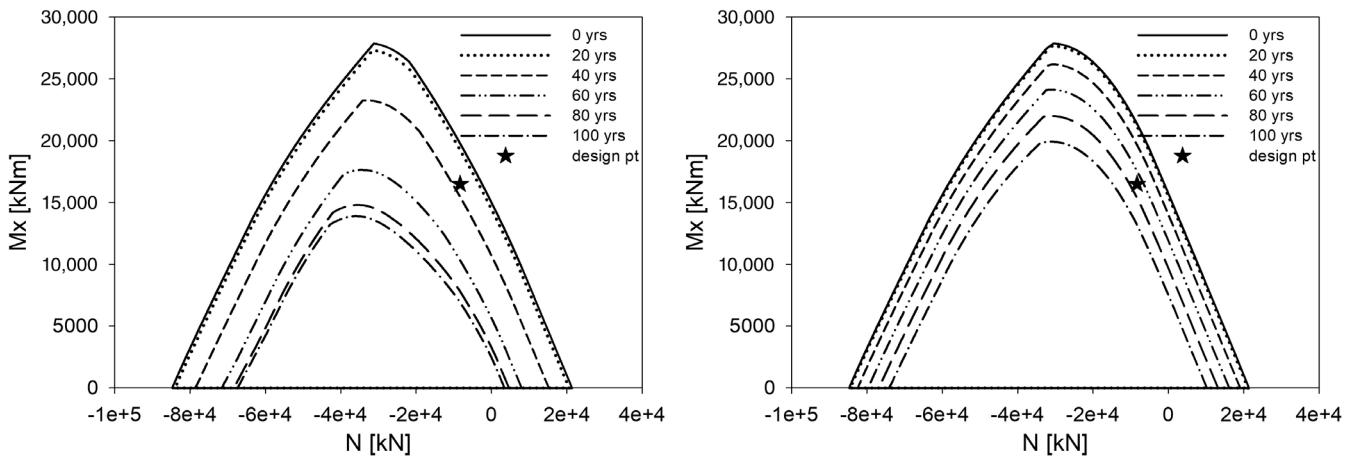


FIGURE 10 Interaction domain  $m_x$ - $N$  of section B due to pitting corrosion considering (left) and neglecting (right) bond reduction effect

deformation before the failure, avoiding sudden collapse of the structure and, therefore, allowing to intervene in advance. Through the moment-curvature diagram, it is

possible to estimate the curvature ductility of a reinforced concrete section. The variation of the RC pier ductility along time is assessed through the construction of moment-

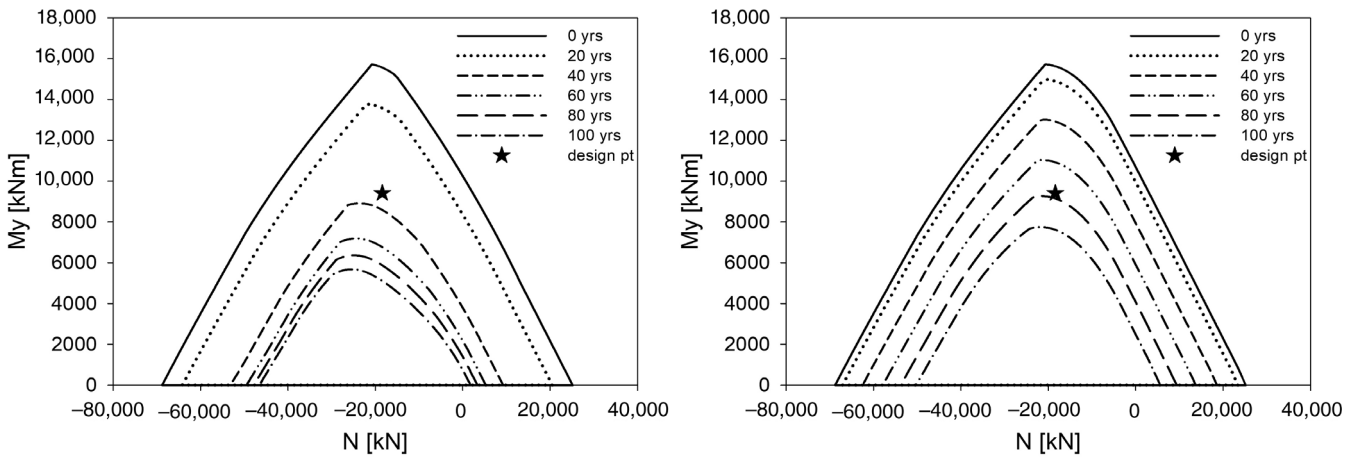


FIGURE 11 Interaction domain my-N of section A due to general + pitting corrosion considering (left) and neglecting (right) bond reduction effect

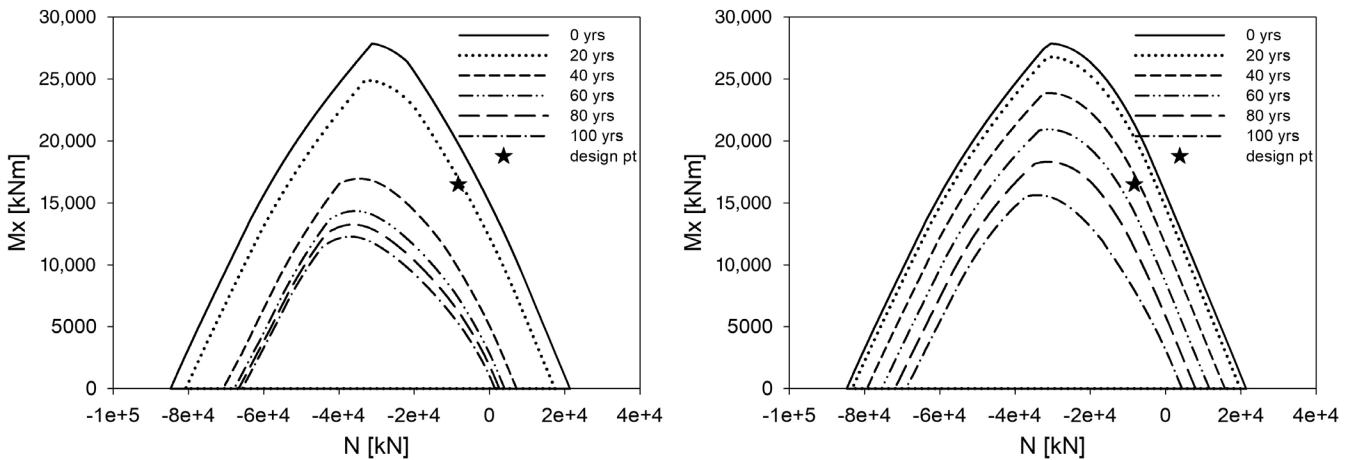


FIGURE 12 Interaction domain mx-N of section B due to general + pitting corrosion considering (left) and neglecting (right) bond reduction effect

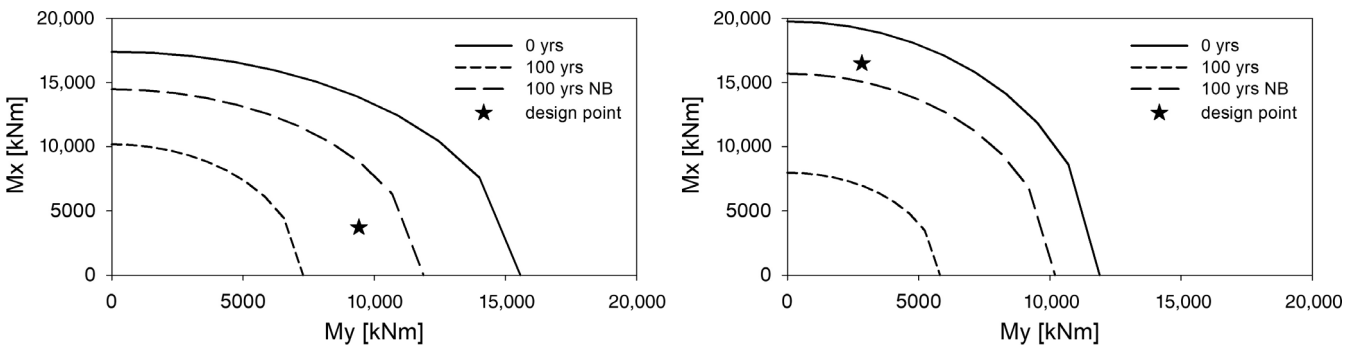


FIGURE 13 Bresler's domain of section A (left) and section B (right) due to general corrosion

curvature diagrams at different corrosion levels. They are computed for a specific value of axial load.

In order to understand how corrosion affects this property, moment-curvature diagrams have been plotted for Section A of the bridge pier for different years. They

have been built first considering the effect of steel area loss only and then, superposing the effect of the bond strength reduction. In the first case (Figures 16–18 left) the curvature ductility slightly increases, while the resistant moment essentially decreases with time. Indeed, the

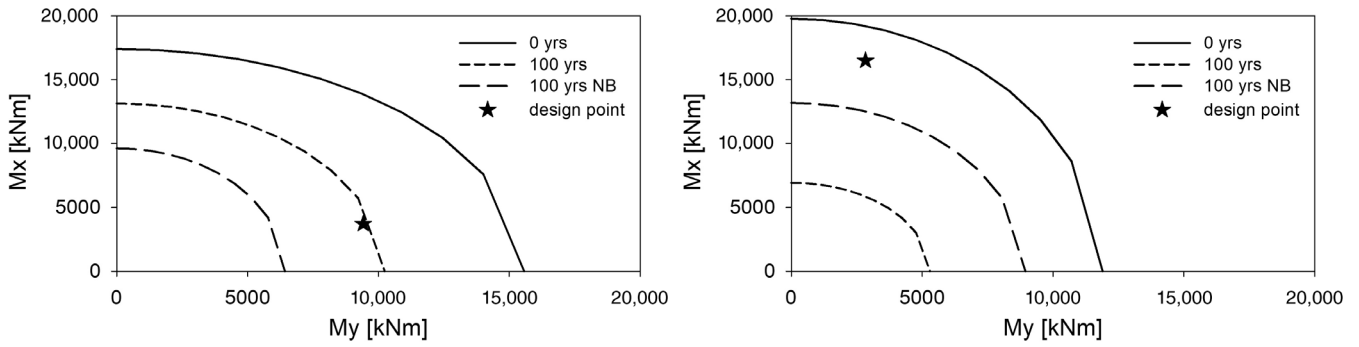


FIGURE 14 Bresler's domain of section A (left) and section B (right) due to pitting corrosion

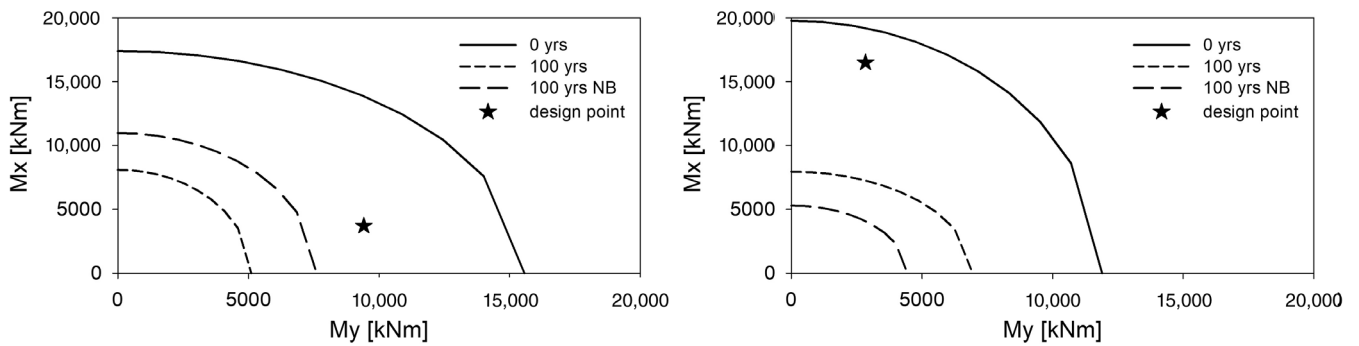


FIGURE 15 Bresler's domain of section A (left) and section B (right) due to general + pitting corrosion

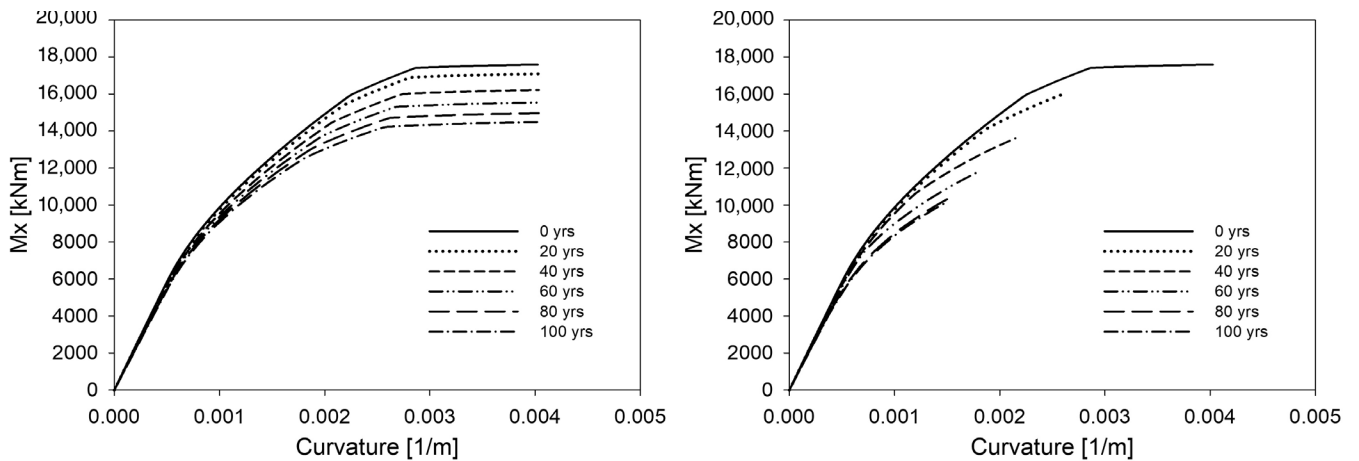


FIGURE 16 Moment - curvature diagram of section ay due to general corrosion, steel area loss effect (left) and steel area loss and bond strength reduction effects (right)

yield curvature undergoes a decrement, because of the decreasing effect of deterioration on the steel yield strength and consequently on the steel yield strain. The slight increase of the ultimate curvature is explicable with the decrease of the amount of steel in the section in time.

In the diagrams representing the cases of section affected by steel area loss and bond deterioration (Figures 16–18 right) ductility losses have been highlighted, exhibiting the fragile response of the RC member. It can be explained by the bond strength decrease. Anyway, it can be noted how during the first

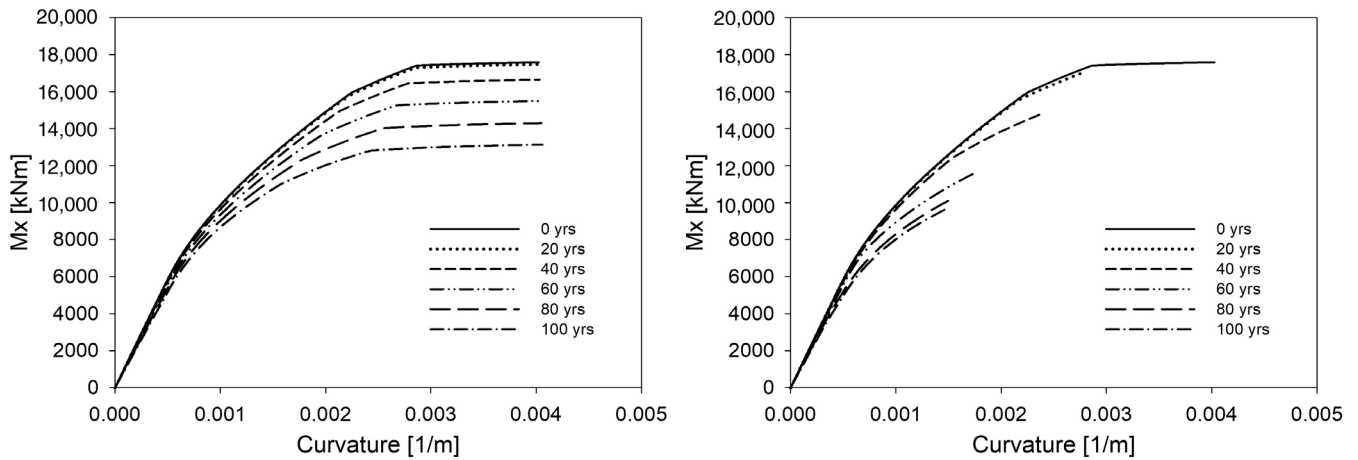


FIGURE 17 Moment - curvature diagram of section ay due to pitting corrosion, steel area loss effect (left) and steel area loss and bond strength reduction effects (right)

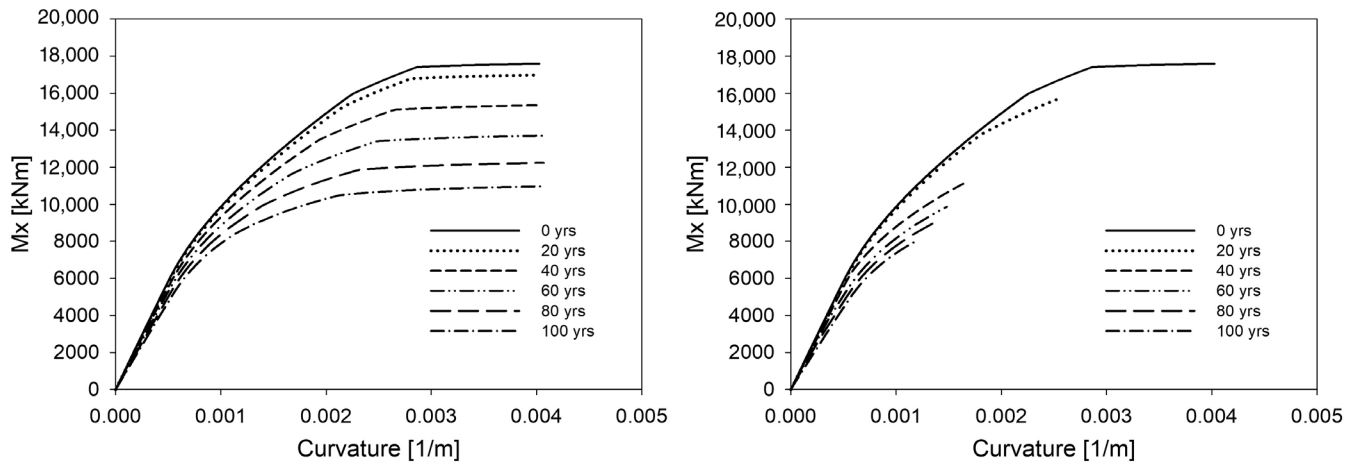


FIGURE 18 Moment - curvature diagram of section ay due to general + pitting corrosion, steel area loss effect (left) and steel area loss and bond strength reduction effects (right)

years of service life, the steel can effectively reach the yielding point. This is related to the time needed for aggressive agents to reach the steel rebars under the concrete cover and to activate the corrosion process (initiation of the propagation phase).

## 7 | VALIDATION OF THE MODEL THROUGH EXPERIMENTAL RESULTS

In order to validate the assumed empirical model to consider the maximum capacity because of bonding stress decrease in the corroded bars, a literature research was carried out with the aim of finding an experimental study whose results could be used for a comparison. The experimental study carried out by Wang and Liang<sup>21</sup> appears to be suitable for this purpose. In fact, they performed

experimental tests on partially corroded concrete columns aimed at determining their load capacities when loaded with combined axial and bending effects. Twelve columns were subjected to an eccentric load by varying both the level of corrosion in the partial length considered, and the position of the corroded area, in the tensile or in the compressive zone. Table 5 reports the parameters of two of the tested columns that were considered suitable for the comparison with the proposed model: they are ZD0 and ZDL350-3. The first one is the non-corroded sample used as comparison to investigate the corrosion effects, while the second is one of the corroded specimens with the partial length located in the tensile zone where a high eccentricity load have been applied. In fact, one of the most important aspects highlighted by the model developed is the brittle failure of the reinforced concrete element due to bond degradation between concrete and steel in the tensile zone. For this reason, the

TABLE 5 Details of the specimens ZD0 and ZDL350-3<sup>21</sup>

Specimens	Cross-section (mm)		Average depth of concrete cover (mm)			Compressive strength of concrete (MPa)	
	Width	Height	Tensile steel	Compressive steel	Eccentric distance (mm)	Chloride-contaminated concrete	Free-chloride concrete
ZD0	203	185	25	30	156.5	-	36
ZDL350-3	205	201	22	41.5	150.5	40	45.3

specimen ZDL350-3 has been chosen among those with the partial length subjected to corrosion in the tensile zone because it is the only one falling due to loss of bond.

Columns were casted using chloride contaminated concrete for the designed partial length and free chloride concrete for the other zones. Sheets have been used to separate the two different regions. After 14 days the specimens have been subjected to accelerated corrosion, connecting the longitudinal bars located in the partial length to the positive terminal of an external power supply and the stainless-steel bar, positioned inside the column during casting, to the negative terminal of the power supply. Wet sack sheets have been used in order to provide moisture and permits to the corrosion process to occur.

Loading tests have been performed, applying eccentric load to the columns using a hydraulic actuator, and after that the specimens have been broken in order to measure the average weight loss of the steel. Table 6 reports the results of the tests in terms of average weight loss of the steel and ultimate load.

The model ARC2010 for bond anchorage assessment in corroded concrete structures has been applied to the two specimens chosen in order to compute the original bond strength, in the case of the uncorroded sample, and the deteriorated bond strength, for the corroded one. The specimens input parameters of the model are reported in Table 7.

Knowing the steel weight loss from tests results, it is possible to compute the equivalent slip. It has been

calculated for two different corrosion levels, the one measured in the top and in the bottom tensile bar of the specimen (the term top and bottom refer to their position during the casting of the column, which was done with the column in horizontal position).

$$S_{eq, stir} (\text{top tensile bar}) = 13.6 * 0.0438 = 0.5957$$

$$S_{eq, stir} (\text{bottom tensile bar}) = 13.6 * 0.0378 = 0.5141$$

Once computed the equivalent slip, it has been used to translate the bond strength - slip curve of the uncorroded specimen and to find the value of the deteriorated bond strength at that specific level of corrosion. Then, the values of the deteriorated bond strength has been compared with the bond strength of the uncorroded column and the percentual reduction has been obtained. According to the hypothesis done, the same reduction will be applied to the steel yield strength (Table 8), assuming null post-yielding stiffness. Let us remember that this yield strength reduction is not real and just a value used to take into account the bond degradation when using standard methods that assume full bond when assessing the sectional response.

Lastly, the parameters have been used for the calculation of the Moment - Curvature diagrams and the corresponding ultimate bending moment under a fixed axial load. They are compared with the results from the test as presented in Table 9.

TABLE 6 Columns test results<sup>21</sup>

Specimens	Average weight loss of the steel (%)						Ultimate load (kN)
	Longitudinal bars				Stirrups		
	Top tensile	Bottom tensile	Top compressive	Bottom compressive	Tensile side	Compressive side	
ZD0	0	0	0	0	0	0	239.1
ZDL350-3	4.38	3.78	1.95	4.31	9.71	4.93	240.1

TABLE 7 Columns test results<sup>21</sup>

	ZD0	ZDL350-3
$f_{cm}$ (MPa)	36	40
$c_s$ (mm)	104	104
$c_x$ (mm)	25	22
$c_y$ (mm)	25	22
$n_t$	2	2
$n_b$	2	2
$c_{clear}$ (mm)	5.8	5.8
$s_t$ (mm)	100	100
$c_{min}$ (section A) (mm)	25	22
$c_{max}$ (mm)	52	52
$k_m$	0	0
$A_s(t)$ (mm <sup>2</sup> )	50	50
$K_{tr}$	0.0279	0.0279

The results obtained show that the model slightly underestimates the bending moment capacity or the reinforced concrete columns (it is in the conservative side), but the results turn out to be consistent with the outcome of the experimental study, with a maximum difference less than 5%. It should be also pointed out that in the case of the undamaged column (ZD0), the error is

already of 2 %. Therefore, only an error of around 3% should be assigned to the proposed model.

## 8 | CONCLUSIONS

The paper aimed to evaluate the effects of bond degradation on corroded reinforced concrete structures. The study is carried out applying the empirical model ARC2010 for bond degradation to the bridge pier designed in a previous research that analyzed the seismic capacity of the RC bridge component considering the steel area loss effect only.

The following conclusions arise:

1. Focusing on the adherence, it is possible to highlight its influence in the determination of the corroded structure service life and its critical role on the results if it is included in the computation or neglected.
2. The bond effect between steel and concrete is essentially related to the characteristics of both materials conditions to be fully exploited: a strong change in the RC element capacity is verified if bond undergoes to degradation. This study confirms the expectations of a drastic reduction in strength capacity and ductility of the bridge pier if bond strength reduction is considered in addition to the steel area loss.

TABLE 8 Bond strength reductions and steel yield strength reductions of bars

Specimens	$W_c$ (%)	$S_{eq}$ (mm)	Bond strength (MPa)	Relative bond strength (%)	Bond strength reduction (%)	Steel yield strength reduction (%)
ZD0	0	0	8.88	100	0	0
ZDL350-3 (uncorroded)	0	0	8.94	100	0	0
ZDL350-3 (corroded-top tensile bar)	4.38	0.59	7	78.3	21.7	21.7
ZDL350-3 (corroded-bottom tensile bar)	3.78	0.51	7.11	79.5	20.5	20.5

TABLE 9 Comparison between ultimate moments from tests and the proposed model

Specimens	Ultimate load from test (kN)	Load eccentricity (mm)	$M_u$ (test) (kNm)	$M_u$ (model) (kNm)
ZD0	239.1	156.5	37.42	36.72
ZDL350-3 (corroded-top tensile bar)	240.1	150.5	36.14	34.4
ZDL350-3 (corroded-bottom tensile bar)	240.1	150.5	36.14	34.8

3. The results obtained in the previous research considering steel area losses only showed an important degradation in the pier strength capacity, with essential reduction of the structure service life. The bond degradation induces a further reduction of the pier strength and an earlier failure of the structure. In detail, focusing on section A, if bond degradation is considered, the reduction of the service life is about 50% and 70% for pitting and general corrosion acting separately and at the same time, respectively. While the service life undergoes about 20% reduction only if general and pitting corrosion act in association and bond reduction effects are neglected. Considering section B and bond degradation effects, a service life reduction of 70% and 80% occurs if pitting and general corrosion act separately and at the same time, respectively. If area loss only is considered, the reduction is about 30% in the cases of general and pitting corrosion acting separately and 60% considering their combined effects.
4. As corrosion progresses, the ductility of RC pier sections is completely lost. Bonding degradation essentially converts the RC pier seismic response from ductile to fragile behavior, potentially inducing the abrupt failure of the structure.
5. The validation of the proposed model through experimental results confirmed its reliability. In fact, comparing the experimental results with the results obtained by applying the model to the specimens used in the tests, a discrepancy on the bending moment capacity of less than 5% was highlighted.

## NOMENCLATURE LIST

$q$	behavior factor
$d(t)$	residual reinforcement diameter
$p(t)$	residual pitting depth
$A(t)$	residual cross-sectional area of steel bar
$d_0$	diameter of the intact reinforcement bar
$R$	amplification factor representing the ratio between maximum and uniform corrosion penetration
$\lambda(t)$	corrosion rate function
$\tau_b$	tangential bond strength (MPa)
$\tau_{b,max}$	maximum value of the tangential bond strength (MPa)
$\tau_{res}$	residual tangential bond strength (MPa)
$s$	slip values with respect to local bond strength
$\tau_{bu,split}$	tangential bond splitting strength (MPa)
$f_{cm}$	mean cylinder compressive strength (MPa)
$c_{clear}$	clear distance between ribs (mm)
$\eta_2$	bond condition parameter
$\phi_m$	diameter of the anchored bar (mm)


$k_m$	confinement coefficient
$c_s$	clear spacing between main bars (mm)
$x, y$	reference directions on the cross-section
$c_x, c_y$	cover in x and y (mm)
$c_{min}$	$\min(c_s/2, c_x, c_y)$
$c_{max}$	$\max(c_s/2, c_x)$
$K_{tr}$	amount of transverse reinforcement
$n_t$	number of legs of confining reinforcement crossing a potential splitting-failure surface
$A_{st}$	cross-sectional area of one leg of a transverse bar ( $\text{mm}^2$ )
$s_t$	longitudinal spacing of confining reinforcement (mm)
$n_b$	number of anchored bars or pairs of lapped bars in the potential splitting surface
$t$	time instant
$S_{eq, stir}$	equivalent slip (mm)
$W_c$	corrosion level (weight loss)

## DATA AVAILABILITY STATEMENT

The data that support the findings of this study are available from the corresponding author upon reasonable request.

## ORCID

Joan R. Casas  <https://orcid.org/0000-0003-4473-4308>

Marco Domaneschi  <https://orcid.org/0000-0002-6077-8338>

## REFERENCES

1. Cairns J, Dut Y, Law D. Structural performance of corrosion-damaged concrete beams. *Mag Concr Res*. 2008;80:359–70.
2. Kabir M, Islam M. Bond stress behaviour between concrete and steel rebar: critical investigation of pull-out test via finite element modeling. *Int J Civ Struct Eng*. 2014;5:80–90.
3. Lundgren K. Bond between ribbed bars and concrete. Part 2: the effect of corrosion. *Mag Concr Res*. 2005;57:383–95.
4. Al-Sulaimani GJ, Kaleemullah M, Basunbul IA, Rasheeduzzafar. Influence of corrosion and cracking on bond behaviour and strength of reinforced concrete members. *ACI Struct J*. 1990; 87(2):220–31. <https://www.concrete.org/publications/internationalconcreteabstractsportal/m/details/id/2732>
5. Zhao Y, Lin H. The bond behaviour between concrete and corroded reinforcement: state of the Art. Sixth international conference on the durability of concrete structures. United Kingdom: Leeds; 2018.
6. Kivell ARL. Effects of bond deterioration due to corrosion on seismic performance of reinforced concrete structures. Master's thesis in faculty of Civil Engineering. University of Canterbury; 2012.
7. Chung L, Jay Kim J, Yi S. Bond strength prediction for reinforced concrete members with highly corroded reinforcing bars. *Cem Concr Compos*. 2008;30:603–11.
8. Coronelli D, Gambarova P. Structural assessment of corroded reinforced concrete beams: modeling guidelines. *J Struct Eng*. 2004;130:1214–24.



9. Coronelli D. Corrosion cracking and bond strength modelling for corroded bars in reinforced concrete. *ACI Struct J.* 2002;99: 267–76.
10. Lin H, Zhao Y. Effects of confinements on the bond strength between concrete and corroded steel bars. *Constr Build Mater.* 2016;118:127–38. <https://www.sciencedirect.com/science/article/abs/pii/S0950061816307632>
11. Chen H, Nepal J. Gamma process modelling for lifecycle performance assessment of corrosion affected concrete structures. *The 2014 World Congress on Advances in Civil, Environmental, and Materials Research.* Busan, Korea: ACEM14; 2014.
12. Fischer C, Ozbolt J. An appropriate indicator for bond strength degradation due to reinforcement corrosion. *VIII International Conference on Fracture Mechanics of Concrete and Concrete Structures FraMCoS-8.* Spain: Toledo; 2013.
13. Yang Y, Nakamura H, Miura T, Yamamoto Y. Effect of corrosion-induced crack and corroded rebar shape on bond behaviour. *Struct Concr.* 2019;20:2171–82.
14. De Gaetano A. Seismic performance of deteriorating concrete bridges. Master's thesis 2019, Politecnico di Torino. Advisors: Marco Domaneschi, Joan R. Casas.
15. Domaneschi M, De Gaetano A, Casas JR, Cimellaro GP. Deteriorated seismic capacity assessment of RC bridge piers in corrosive environment. *Struct Concr.* 2020;21:1823–38.
16. Coronelli D, Blomfors M, Zandi K, Lundgren K. Engineering bond model for corroded reinforcement. *Eng Struct.* 2018;156:394–410.
17. NTC. Norme tecniche per le costruzioni. Decree of the Minister of the Infrastructures 14; 2018.
18. Val DV, Stewart MG. Life-cycle cost analysis of reinforced concrete structures in marine environments. *Struct Saf.* 2003;25: 343–62.
19. Cui F, Zhang H, Ghosn M, Xu Y. Seismic fragility analysis of deteriorating RC bridge substructures subject to marine chloride-induced corrosion. *Eng Struct.* 2018;155:61–72.
20. FIB, Model Code for Concrete Structures 2010. Federation Internationale du Beton. Lausanne, 2010.
21. Wang XH, Liang FY. Performance of RC columns with partial length corrosion. *Nucl Eng Des.* 2008;238(12):3194–202. [https://www.sciencedirect.com/science/article/pii/S0029549308004500?casa\\_token=nA45SUDQrI8AAAAA:ny8Bo09v\\_JO0Utxzi6CarE-oi\\_gMT6CJivZexx\\_FmDeeqrZ396TU0XhpfNohUJE2IWdtXpJBbA](https://www.sciencedirect.com/science/article/pii/S0029549308004500?casa_token=nA45SUDQrI8AAAAA:ny8Bo09v_JO0Utxzi6CarE-oi_gMT6CJivZexx_FmDeeqrZ396TU0XhpfNohUJE2IWdtXpJBbA)

## AUTHOR BIOGRAPHIES



**Mara Bartolozzi**, Department of Structural, Geotechnical and Building Engineering, Politecnico di Torino, Turin, Italy. Email: [s264896@studenti.polito.it](mailto:s264896@studenti.polito.it)



**Joan R. Casas**, Department of Civil and Environmental Engineering, Universitat Politècnica de Catalunya, Barcelona, Spain. Email: [joan.ramon.casas@upc.edu](mailto:joan.ramon.casas@upc.edu)



**Marco Domaneschi**, Department of Structural, Geotechnical and Building Engineering, Politecnico di Torino, Turin, Italy. Email: [marco.domaneschi@polito.it](mailto:marco.domaneschi@polito.it)

**How to cite this article:** Bartolozzi M, Casas JR, Domaneschi M. Bond deterioration effects on corroded RC bridge pier in seismic zone. *Structural Concrete.* 2021;1–16. <https://doi.org/10.1002/suco.202000681>